International Journal of Thermophysics, Vol. 16, No. 5, 1995

The Process of Heat and Mass Transport at the Critical Point of Pure Fluids[1]

J. Straub,[2,3] L. Eicher,[2] and A. Haupt[2]

The effects of fast isentropic temperature propagation, called the "piston effect," or "critical speeding up," and slow mass diffusion, called "critical slowing down," are investigated. A temperature propagation experiment in a spherical cell filled with pure SF_6 at critical density was performed during the Second German Spacelab Mission D2 in 1993. The results evidently confirm the presence of the piston effect both in the one-phase region and in the two-phase region. The numerical simulations are in remarkable good quantitative agreement with the experimental results.

KEY WORDS: critical phenomena; D2 Mission; density relaxation; microgravity; SF_6; temperature relaxation.

1. INTRODUCTION

Experiments in near-critical pure fluids suffer under very slow relaxation. This effect is called "critical slowing down." The relatively fast temperature equilibration observed on earth ($1g$) was explained by gravity-induced buoyancy convection. However, in the first experiment performed under microgravity (μg) with a ballistic rocket [1], where convection was excluded, the temperature propagation was still very fast. Onuki et al. [2] explained this by fast isentropic temperature propagation and Boukari et al. presented a numerical solution [3] and an experimental test on earth [4]. They call the effect "critical speeding up." This model reveals that the high compressibility of a critical fluid and the finite volume of the sample

[1] Paper presented at the Twelfth Symposium on Thermophysical Properties, June 19–24, 1994, Boulder, Colorado, U.S.A.

[2] Institute A for Thermodynamics, Technical University Munich, Arcisstr. 21, 80333 Munich, Germany.

[3] To whom correspondence should be addressed.

0195-928X/95/0900-1051$07.50/0

cell cause this fast isentropic temperature change. This process is completely different from heat transfer by conduction. Recent experiments [5, 6] have confirmed these considerations qualitatively. In this paper we present a quantitative experiment carried out during the Second German Spacelab Mission D2 in 1993. A spherical cell filled with pure SF_6 at critical density was heated pulsewise and the temperature propagation in the fluid was monitored. Numerical simulations using the experimental boundary conditions are in very good agreement with the experiments.

2. TEMPERATURE PROPAGATION

The Fourier equation generally used for the description of heat conduction is valid only for incompressible substances. A critical fluid, however, is highly compressible, and therefore the complete hydrodynamic equations have to be considered. Zappoli et al. [7] presented the first solution for a van der Waals fluid. However, solving the complete set of hydrodynamic equations with an equation of state for a real fluid requires an extremely long computation time. Since the sound velocity is still high close to the critical point (e.g., 50 $m \cdot s^{-1}$ at $T - T_c = 0.01$ K), in Ref. 3 the momentum equation is reduced by the assumption that the pressure in the system is constant over the whole sample volume and therefore only time dependent. Neglecting the velocities in the fluid, the conservation of energy is described by

$$\frac{\partial T}{\partial t} - \left(1 - \frac{c_V}{c_P}\right)\left(\frac{\partial T}{\partial p}\right)_\rho \frac{\partial p}{\partial t} = \frac{1}{\rho c_P} \nabla(\lambda \nabla T) \tag{1}$$

where λ represents the thermal conductivity and t the time. From conservation of mass and thermodynamic relations follows

$$\frac{\partial p}{\partial t} = \frac{\int_V \rho \alpha_P (\partial T/\partial t)\, dV}{\int_V \rho \chi_1\, dV} \tag{2}$$

where α_P is the isobaric expansion coefficient and χ_T is the isothermal compressibility. Based on the analytic solution presented in Ref. 2, we developed an equation which describes analytically the temperature response in the fluid caused by a temperature quench or rise from the initial temperature T_0 to the final temperature T_W at the wall:

$$\frac{T_W - T(x, t)}{T_W - T_0} = \exp\left[-\left(\frac{c_P}{c_V} - 1\right)\sqrt{D_{th}}\frac{A}{V}\sqrt{\frac{4}{\pi}}\, t^{1/2}\right] \operatorname{erfc}\left(\frac{x}{2\sqrt{D_{th} t}}\right) \tag{3}$$

Here A is the heating area of the sample, V the volume, $T(x, t)$ the actual temperature in the fluid, and D_{th} the thermal diffusivity. This equation

illustrates that an increasing ratio A/V accelerates the temperature change in the bulk. This fact must be considered for the design of an experiment. As $(c_P/c_V)\sqrt{D_{th}} \sim \tau^{-0.8}$ diverges for $\tau = |(T-T_C)/T_C| \to 0$, the temperature propagation becomes faster approaching the critical point. For $x/2\sqrt{D_{th}t} > 2$ the erfc tends to unity, and Eq. (3) describes the isentropic temperature change in the bulk fluid.

3. THE D2 EXPERIMENT

For the experiment on temperature propagation during D2 we used the calorimeter setup described in Ref. 8, however, now in an adiabatic mode. The spherical cell (inner diameter R, 9.6 mm; wall thickness, 0.4 mm), which was equipped with a heater on the outer surface, was used. So the complete wall of the cell was the heating area and we obtained a large ratio of $A/V = 3/R$. At 39 temperatures in the range $0.03\ \text{K} < |T-T_C| < 5.25\ \text{K}$, the cell was heated for 10 s with a power of 3.85 mW. The temperature response was monitored with four thermistors (diameter, 0.35 mm; time constant, 0.1 s) in time steps of 0.6 s. One thermistor was fixed at the outer surface of the cell; three were in the fluid at different distances from the wall (3.2, 6.0, 8.4 mm). Each heat pulse caused a temperature increase in the cell between 8 and 15 mK, depending on the distance from T_C.

4. NUMERICAL SIMULATIONS

We performed numerical simulations of all experimental runs based on Eqs. (1) and (2), which have to be solved iteratively for the two variables time and location. As the time variable boundary condition we used the recorded temperature rise of the cell wall.

5. RESULTS AND DISCUSSION

In Fig. 1, two experimental runs performed above T_C are compared. Obviously the temperature propagation becomes faster upon approaching T_C. For $T-T_C = +0.1$ K and for all temperatures closer to T_C, no significant temperature difference between wall and fluid could be observed. For both runs there are no perceptible temperature differences among the three thermistors in the fluid. The simulations yield the same result: Temperature gradients exist only in a very thin boundary layer near the wall, which after 10 s (at the end of the heat pulse), has a thickness of 0.25 mm at $T-T_C = +0.1$ K and 1.0 mm at $T-T_C = +4.75$ K. The bulk fluid is isothermal.

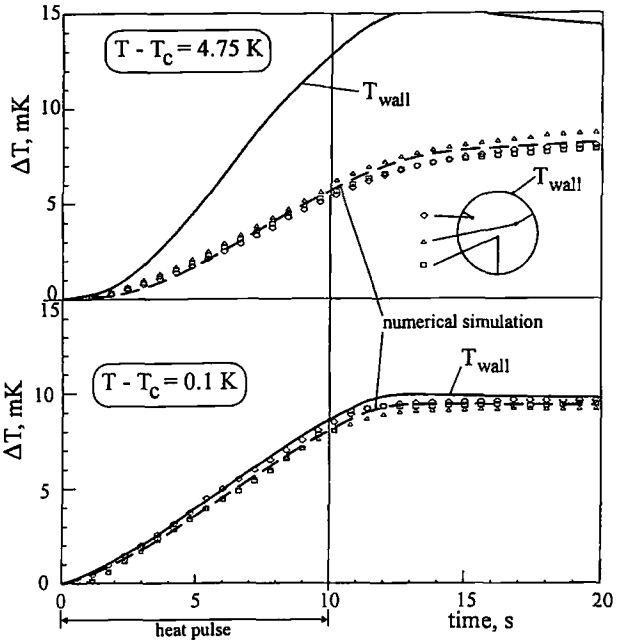

Fig. 1. Comparison of two typical experimental runs above T_C (0.1 and 4.75 K). The temperature change in the fluid (triangles, squares, diamonds) and on the wall (solid line) was monitored in time steps of 0.6 s. The numerical simulation (dashed line) used the wall temperature as the boundary condition.

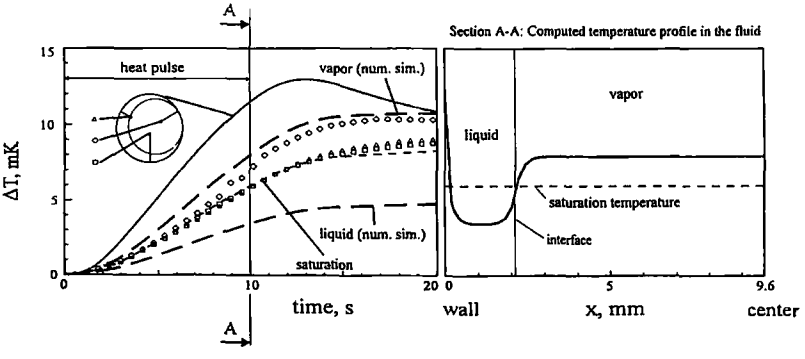

Fig. 2. Experimental run 2.25 K below T_C. Section A-A shows the temperature distribution versus distance x from the wall obtained from the numerical simulations.

Below T_C (Fig. 2), however, the heat pulse obviously causes temperature gradients in the fluid. For the simulations below T_C we assumed a symmetrical phase distribution in the cell filled with critical density. The vapor bubble, taking half of the cell volume in the center, is surrounded by a liquid layer at the wall of about 2-mm thickness.

According to the numerical simulations the temperatures of two thermistors follow the predicted temperature course of the interface, and the temperature of the thermistor at $x = 6.0$ mm corresponds to the predicted one for the vapor (see Fig. 2). This indicates that the real phase distribution during this experiment was not symmetrical as assumed in the simulation.

The calculated temperature responses of the liquid and the vapor differ strongly due to the different thermodynamic properties of the two phases (see Section A-A in Fig. 2). The temperature–entropy diagram (Fig. 3) explains this effect: Starting from the saturation line (1), a thin liquid boundary layer is heated up into the metastable region and expands (2), then the saturated bulk fluid (1)—both liquid and vapor—is compressed isentropically and heated up (3). Due to the asymmetry of the isobars in the T, s diagram, the temperature increase of the vapor is larger than that of the liquid.

The vapor is superheated and the liquid subcooled; phase transition with mass transport occurs only at the interface.

During cooling, the behavior of the system is different: Isentropic expansion brings both saturated bulk phases (1) into the metastable region (3), so bubbles in the liquid and droplets in the vapor are nucleated (4). Due to the latent heat consumed and released by the subsequent growth of these bubbles and droplets, respectively, the surrounding fluid comes back to saturation (5). This phase transition effect continues as long as the wall temperature decreases, and therefore a disperse phase distribution is obtained during cooling ramps. This was observed in our early TEXUS experiments [1], in the Critical Point Facility (CPF) during the IML-1 Mission, and during the USMP-2 Mission [9] and is observable on earth, too. During cooling, continuous nucleation of bubbles in the liquid and droplets in the vapor is observed simultaneously.

Figure 4 shows the results of all μg runs and some $1g$ runs. Under μg the numerical simulation is in very good agreement with the experiment for all runs above T_C.

Below T_C the measured temperature increase is between the value calculated for liquid and that for vapor. In most cases it corresponds to the saturation temperature, which means that the thermistors were close to the interface. So we conclude that the real phase distribution in the sample was not symmetrical because the wetting conditions at the thermistors squeezed

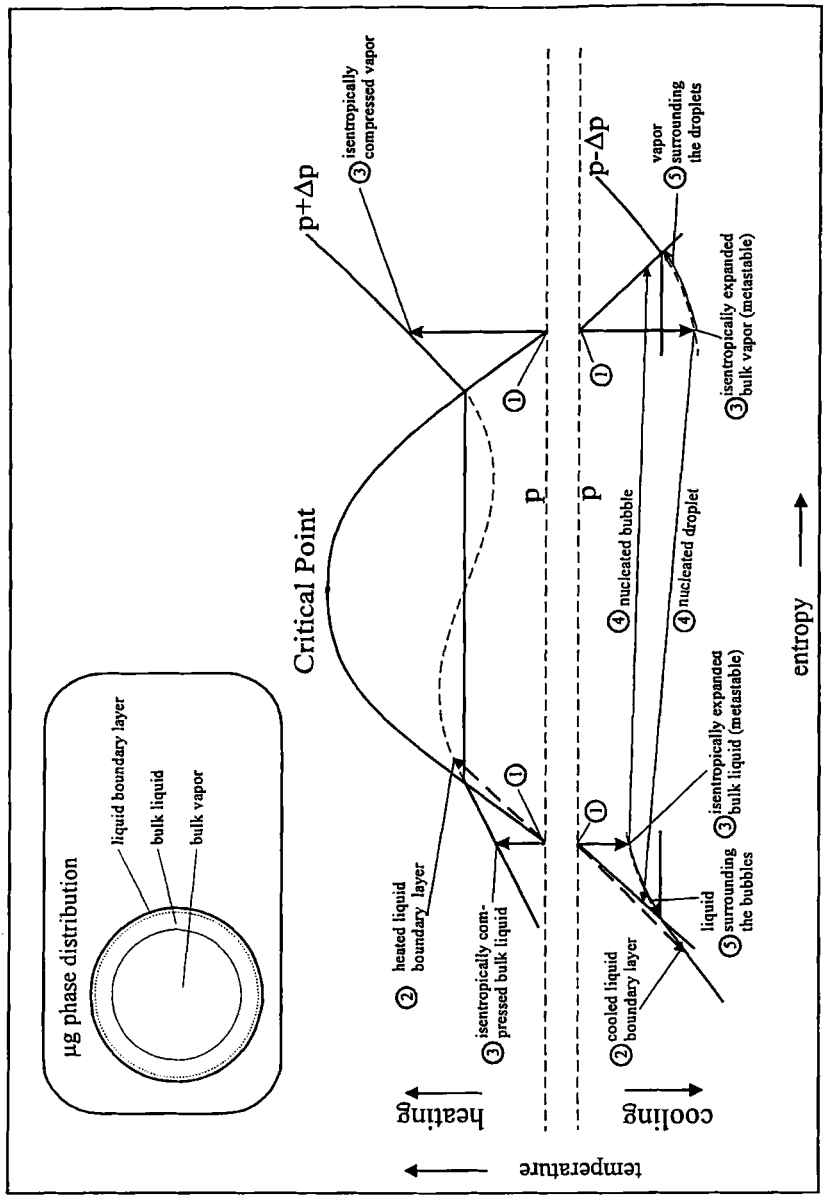

Fig. 3. Effect of heating and cooling, respectively, in the two-phase region, schematically explained in a temperature–entropy diagram.

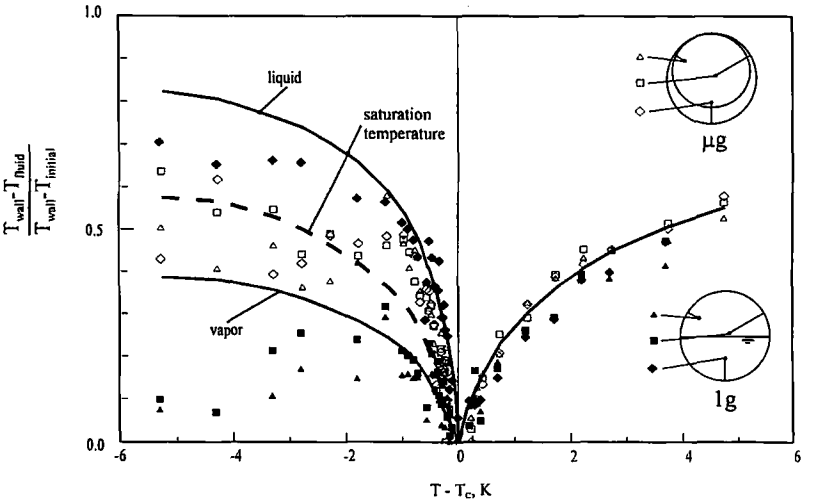

Fig. 4. Observed and computed temperature differences at the end of the heat pulse as a function of temperature. Open symbols, μg experiments; filled symbols, $1g$ experiments; solid lines, numerical simulation.

the bubble into one of the hemispheres established by the wires of the thermistors, which were mounted in a central plane of the spherical cell. We have confirmed this in drop tower experiments recently conducted at ZARM in Bremen (not published yet).

Between $T - T_C = -1$ K and $T = T_C$ the measured temperature change corresponds to the behavior predicted for the liquid. This effect may be explained by perfect wetting near the critical point, as described in Ref. 10.

During the $1\,g$ experiments the phase distribution is obvious and we know which thermistor was in the liquid and which was in the vapor. Evidently the measured temperature difference between liquid and vapor is equal to the predicted difference. At $|T - T_C| > 1$ K the temperature difference between wall and fluid is smaller than the predicted one. This may be caused by the onset of convection.

6. SUMMARY

Our experiments evidently confirm the presence of fast isentropic temperature equilibration both in the one-phase region and in the two-phase region. The numerical simulations performed are in very good agreement with the experiments and quantitatively confirm the theory.

Even at 1 g the isentropic temperature propagation is dominant. The influence of convection is noticeable only for $|T - T_c| > 1$ K. The predicted different temperature response for liquid and vapor is observed in the experiments.

ACKNOWLEDGMENTS

This research is supported by Deutsche Agentur für Raumfahrtangelegenheiten (DARA), Project Number 50 QV 8948. The authors want to thank the crew of the Space Shuttle Columbia STS 55, the responsible persons of the company Kayser-Threde, Munich, the operations control team of DLR and NASA, and all colleagues and students for their outstanding engagement in the D2 experiment HPT-HYDRA.

REFERENCES

1. K. Nitsche and J. Straub, in *Proceedings of the Sixth European Symposium on Material Sciences Under Microgravity Conditions, Bordeaux, France, 1986* (European Space Agency, Paris, 1987), Vol. SP-256, p. 109.
2. A. Onuki, H. Hao, and R. A. Ferrell, *Phys. Rev. A* **41**:2256 (1990).
3. H. Boukari, J. N. Shaumeyer, M. E. Briggs, and R. W. Gammon, *Phys. Rev. A* **41**:2260 (1990).
4. H. Boukari, J. N. Shaumeyer, M. E. Briggs, and R. W. Gammon, *Phys. Rev. Lett.* **65**:2654 (1990).
5. H. Klein, G. Schmitz, and D. Woermann, *Phys. Rev. A* **43**:4562 (1991).
6. P. Guenoun, B. Khalil, D. Beysens, F. Kammoun, B. LeNeindre, Y. Garrabos, and B. Zappoli, *Phys. Rev. E* **47**:1531 (1993).
7. B. Zappoli, D. Bailly, Y. Garrabos, B. LeNeindre, and D. Beysens, *Phys. Rev. A* **41**:2264 (1990).
8. J. Straub, A. Haupt, and L. Eicher, *Int. J. Thermophys.* **16**:1033 (1995).
9. R. W. Gammon, personal communication (1994).
10. M. R. Moldover and R. W. Gammon, *J. Chem. Phys.* **80**(1):528 (1984).